

# Nondestructive Spent Fuel Assay Using Nuclear Resonance Fluorescence

B. J. Quiter<sup>a</sup>, B. A. Ludewigt<sup>b</sup>, V. V. Mozin<sup>a</sup>, S. J. Tobin<sup>c</sup>

## Abstract

Quantifying the isotopic composition of spent fuel is an important challenge and essential for many nuclear safeguards applications, such as independent verification of the Pu content declared by a regulated facility, shipper/receiver measurements, and quantifying isotopic input masses at a reprocessing facility. As part of the Next Generation Safeguards Initiative, NA-241 has recently funded a multilab/university collaboration to investigate a variety of nondestructive methods for determining the elemental Pu mass in spent fuel assemblies. Nuclear resonance fluorescence (NRF) is one of the methods being investigated. First modeling studies have been performed to investigate the feasibility of assaying a single fuel pin using a bremsstrahlung photon source. MCNPX modeling results indicate that NRF signals are significantly more intense than the background due to scattered interrogation photons even for isotopes with concentrations below 1%. However, the studies revealed that the dominant contribution to the background is elastic scattering, which is currently not simulated by MCNPX. Critical to this effort, we have added existing NRF data to the MCNPX photonuclear data files and are now able to incorporate NRF physics into MCNPX simulations. Addition of the non-resonant elastic scattering data to MCNPX is in progress. Assaying fuel assemblies with NRF poses additional challenges: photon penetration through the assembly is small and the spent fuel radioactive decay and neutron activity lead to significantly higher backgrounds. First modeling studies to evaluate the efficacy of NRF for assaying assemblies have been initiated using the spent fuel assembly library created at the Los Alamos National Laboratory (LANL).

## 1. Introduction

The aim of nuclear safeguards is to assure that weapons-usable material is not diverted from civilian nuclear programs to weapons programs. An effective way to safeguard these materials contained in spent fuel is to quantify the concentrations of fissile isotopes before any materials handling activities, such as transporting fuel, reprocessing, and also while it is stored. Through Next Generation Safeguards Initiative, NA-241 has recently funded a multilab/university collaboration to investigate a variety of nondestructive methods for determining the elemental Pu mass in spent fuel assemblies[1]. As part of this collaboration, isotopic non-destructive analysis of spent nuclear fuel via nuclear resonance fluorescence (NRF) is being investigated. NRF is a unique approach to spent fuel assembly assay because it provides signatures that can quantify the concentration of an isotope – or multiple isotopes – within an assay volume.

NRF has been a known physics phenomenon for over 40 years [2]. Past interest was devoted to nuclear structure studies. More recently, NRF has been identified as a promising technology for the assaying of materials. In the past several years, motivated by the potential application to the screening of cargo for nuclear weapons materials, NRF cross section have been measured for <sup>239</sup>Pu and <sup>235</sup>U [3,4].

<sup>a</sup>University of California, Berkeley

<sup>b</sup>Lawrence Berkeley National Laboratory

<sup>c</sup>Los Alamos National Laboratory

NRF is the process in which a nucleus absorbs a photon and is excited to a specific excited state that subsequently de-excites by emission of one or more  $\gamma$ -rays. By measuring the energies of  $\gamma$ -rays emitted during de-excitation of an NRF state within a medium, one can uniquely identify the presence of the isotope whose state was observed. If the assay geometry and the strength of a measured NRF transition are known, the intensity of a measured NRF signal can be used to quantify the concentration of the isotope within a material. This makes NRF a potentially attractive non-destructive analysis method for spent fuel and other nuclear materials.

The following sections discuss modeling efforts applied to NRF assay methods. These efforts include in-depth investigation of the direct measurement NRF  $\gamma$ -rays emitted from a single fuel pin irradiated by a bremsstrahlung spectrum (section 2). This investigation involved modeling photon transport in the Monte Carlo radiation transport code MCNPX[5]. NRF data has been added to the MCNPX datafiles, enabling the program to simulate NRF interactions (section 3.1). During the modeling studies, it was recognized that MCNPX does not accurately calculate photon transport that contributes to the background for measurement of the NRF signal. Evidence to this is presented as well as a proposal to alleviate the problem (section 3.2). Finally, the extension of the modeling studies to spent fuel assemblies and measurement of the transmitted photon spectra is discussed (section 4).

## **2. Modeling of NRF Measurement of Spent Fuel Pin**

An NRF measurement can be performed using a bremsstrahlung photon beam to induce NRF in the constituents of a spent fuel pin and measuring the emitted photon spectrum at a backward angle with a high energy resolution  $\gamma$ -ray detector, i.e. a high purity germanium (HPGe) detector. The intensity of a measured NRF line in the spectrum corresponds to the amount of the emitting isotope within the spent fuel pin. Such a setup was studied in order to assess the feasibility of using NRF for measuring isotopic content. This study focused on determining the sensitivity for measuring  $^{235}\text{U}$  in spent fuel because the best experimental NRF data were available for this isotope [3]. More recently, NRF cross sections have been measured for  $^{239}\text{Pu}$  [4]. The measured NRF cross sections of  $^{239}\text{Pu}$  were measured to be about a factor of three lower and have slightly higher energies than for  $^{235}\text{U}$ . The conclusions from the  $^{235}\text{U}$  case can be appropriately scaled and applied to the measurement of  $^{239}\text{Pu}$ .

The geometry used in the modeling study is shown in figure 1. The bremsstrahlung photons are generated by an electron beam in a converter foil and collimated onto the fuel pin. The  $\gamma$ -ray detector views the irradiated section of the fuel pin through a collimation borehole in the shielding block at a backward angle. The electron beam energy of 2 MeV and the conversion target, a 4.5 mm thick tungsten slab were optimized for measuring the 1.733 MeV NRF resonance of  $^{235}\text{U}$ . The interrogating bremsstrahlung spectrum is computed in MCNPX by simulating the monoenergetic electron beam impinging on the converter and tallying the generated photon flux into discrete angular bins.

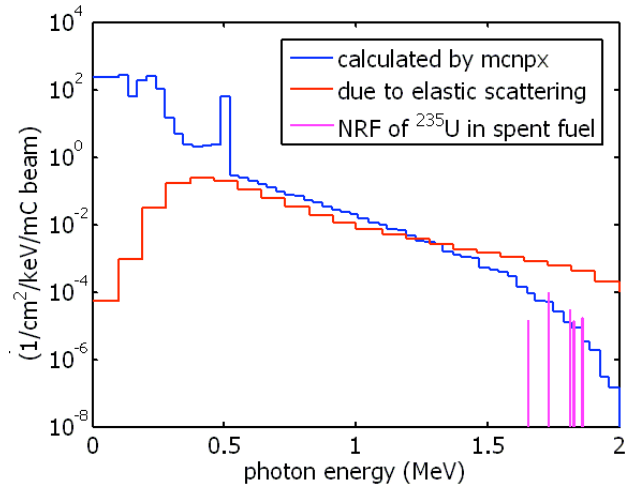
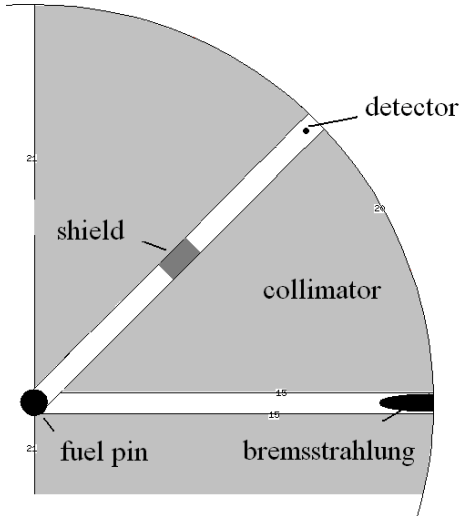


Figure 1. Schematic overview of studied NRF assay geometry, with longitudinal axis of fuel pin normal to depicted plane.

Figure 2. Calculated contributions to photon spectrum at detector location for assay of a spent fuel pin containing 0.41%  $^{235}\text{U}$ . In this calculation no shielding is present between the target and the detector location.

Only photons leaving the bremsstrahlung converter within  $1^\circ$  of the initial electron direction were impinged upon the spent fuel target. Bremsstrahlung outside of the  $1^\circ$  angular acceptance was absorbed by the tungsten collimator. It was determined that with 45 cm of tungsten between the bremsstrahlung converter and the detector location, only a negligible amount of photons reach the detector by penetrating through the tungsten.

The intensity of the NRF signal from the 1.733 MeV resonance of  $^{235}\text{U}$  from a spent fuel pin with  $^{235}\text{U}$  constituting 0.4% of the actinide mass and a 0.5 cm radius was calculated and compared to the intensity of the non-resonantly scattered photons computed by MCNPX. The calculated resonant and non-resonant fluences at the detector location are shown in figure 2. For a meaningful estimate of the NRF signal to background ratio the detector's energy resolution, 3 keV for an HPGe detector at 1.7 MeV, must be taken into account by comparing the integrated NRF peak to the background integrated over the detector's energy resolution width. As can be seen for the accordingly scaled NRF lines in figure 2 the NRF signal for  $^{235}\text{U}$  at 0.4% of the actinide mass is stronger than the background fluence calculated with MCNPX. While this result was initially very encouraging, further examination determined that MCNPX does not simulate important processes that contribute to the background. In particular, it does not include a complete treatment of coherent scattering which would allow for photons to be scattered into all possible angles as discussed in section 3.2.

To add the major part of the photon physics omitted by MCNPX, Rayleigh scattering cross sections tabulated in the RTAB database [6] were folded with the interrogating bremsstrahlung spectrum and geometrically attenuated. The resulting photon flux (labeled "elastic scattering"), also shown in figure 2, is significantly higher at NRF energies than both the MCNPX-computed non-resonant flux and the flux due to NRF of  $^{235}\text{U}$ . These results indicate that the direct measurement of NRF photons at backwards angles may not be an effective NDA method for assaying of spent fuel. Section 4

discusses an indirect measurement technique that may lead to improved signal-to-background ratios.

Another background component in the case of spent fuel that has to be overcome is the radioactive background from the fission products. It is critical for the NRF assay method that the NRF energies are above 1.6 MeV since fuel that has cooled for approximately 10 years predominantly emits lower energy  $\gamma$ -rays. Higher energy lines, primarily due to  $^{154}\text{Eu}$  (8.93 yr half-life) and  $^{150}\text{Eu}$  (36.9 yr half-life), are about 3 orders of magnitude less intense than  $\gamma$ -rays near 1.6 MeV, and these are another 3 orders of magnitude less intense than 662 keV  $\gamma$ -rays from  $^{137}\text{Cs}$ . First estimates indicate that NRF  $\gamma$ -rays from  $^{235}\text{U}$  (at 0.4% of actinide content) are of comparable intensity to the fission product background for a 1 mA bremsstrahlung source.

### 3. MCNPX for Modeling NRF Assay

It became evident in our initial study of NRF for spent fuel assay that MCNPX needed additional capabilities to become a useful tool for modeling NRF responses and background.

#### 3.1 Adding NRF to MCNPX

In order to be able to model the NRF response in MCNPX measured NRF data were added to the photonuclear evaluated nuclear data files (ENDF) and were converted to ACE files for use in MCNPX [7]. To maintain compatibility with existing data processing codes such as NJOY [8], cross sections for NRF interactions have been added as pointwise data and characteristic NRF  $\gamma$ -rays are added as secondary particles emitted by the reaction. The energy width between consecutive data points was selected to be a minimum of 2 eV. This format is necessary because the pointwise ENDF format only allows 6 digits after the decimal place, thus above 1 MeV, an energy point in the ENDF format only has precision to 1 eV. Most NRF resonances have natural linewidths on the order of milli-eV (meV). To describe NRF resonances using such a coarse energy scale, the resonances were Doppler broadened assuming a temperature (T) of 300K. The resulting resonance form is due to Maxwell-Boltzmann statistics:

$$\sigma_D(E) = \int \sigma(E)dE \frac{1}{E_0} \sqrt{\frac{mc^2}{\pi kT}} \exp\left(\frac{-(E - E_0)^2}{E_0^2 kT / mc^2}\right) \quad (1)$$

This form more closely resembles the shape of NRF resonances experienced by incident photons because thermal motion of atoms within materials causes the photons to experience a Doppler-shifted resonance.

Similar to the implementation of NRF cross sections, the energies of emitted NRF photons are entered into ENDF pointwise, and the multiplicity for photon emission is defined for each resonance. These data ensure that photon emission is correct *on average*, but the energies of emitted  $\gamma$ -rays and  $\gamma$ -ray multiplicities are sampled independently. Because this sampling is uncorrelated, coincident  $\gamma$ -ray emissions are not accurately implemented in the database and thus simulations in MCNPX will also not feature correlated  $\gamma$ -rays.

E (keV)	Angle
74.4	180°
105	90°
194	45°
853	10°
1733	4.9°
2423	3.5°

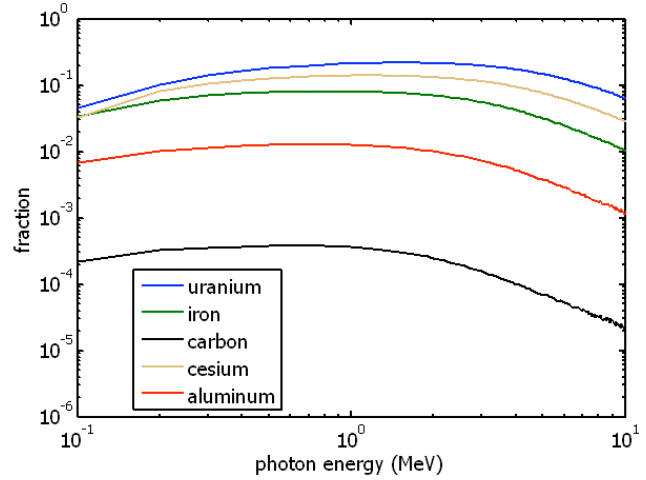


Table 1. Maximum scattering angles computed by MCNPX for Rayleigh scattering of photons.

Figure 3. Fraction of Rayleigh scattering cross section that corresponds to a momentum transfer,  $\nu \geq 6 \text{ \AA}^{-1}$ .

### 3.2 Rayleigh Scattering in MCNPX

The physics treatment of coherent scattering in MCNPX remains the same as that initially implemented in its precursor code MCP in 1973 [9]. The angular differential coherent scattering cross section is given by:

$$\sigma_{cs} d\mu = C(Z, \nu) T(\mu) d\mu \quad (2)$$

In equation 2,  $\mu$  is the cosine of the scattering angle,  $C(Z, \nu)$  is the atomic form factor, and  $T(\mu)$  is the Thompson scattering cross section given by  $T(\mu) = \pi r_e^2 (1 + \mu^2)$ , where  $r_e$  is the classical electron radius. The atomic form factor accounts for the electronic structure of the scattering atom. Each form factor is a function of the element ( $Z$ ) that scatters the photon, and of the momentum that must be transferred to the scattering electron during the scattering process. For a fixed scattering atom and photon energy  $C$  becomes only a function of the scattering angle.

The momentum transfer,  $\nu$ , for a given scattering event is tabulated in units of inverse length by making the following conversion:

$$\nu = \sqrt{\frac{1 - \mu}{2}} \frac{E}{hc} = 57.03 \sqrt{1 - \mu} E \quad (3)$$

$\nu$  is in units of inverse angstroms when  $E$ , the scattering photon energy, is in units of MeV. Distributed versions of the code MCNP have a fixed array on which  $\nu$  is tabulated. Despite the fact that the evaluated photon data library (EPDL) [10] now tabulates  $\nu$  up to  $1 \times 10^{11} \text{ \AA}^{-1}$ , the maximum value of  $\nu$  that is allowed in MCNP is  $6 \text{ \AA}^{-1}$ . Figure 3 presents the fraction of the coherent scattering cross section that is truncated by this cutoff versus photon energy for various scattering mediums, and table 1 lists maximum scattering angles that are simulated by MCNP due to this cutoff.

To confirm that MCNPX's handling of elastic photon scattering was incomplete, we have simulated several elastic photon scattering experiments conducted by Hardie et. al. and Rullhausen et. al. [11, 12, 13]. In these experiments, radioactive sources emitting nearly monoenergetic  $\gamma$ -rays were placed in a shielded lead container with an opening directed towards thin sheets of the target material. A variety of materials, including uranium were studied as scattering targets. Lithium drifted germanium detectors were used to measure the photons scattered from the scattering targets. In all experiments,

photon peaks from elastic scattering were observed. Our MCNPX simulations do not show these peaks, but instead a very low-intensity continuum due to bremsstrahlung from photoelectrons induced in the target foils. Based on MCNPX simulations of the Hardie paper, the limit of the elastic scattering cross section for 60 degree scattering of 1.332 MeV photons incident upon uranium is less than 300nb/str, whereas the authors reported measuring a cross section of 430  $\mu$ b/str.

Altering the array of momentum transfers on which the form factor is defined is a trivial task. However, the data processing codes that are used to format data for use in MCNPX would also require modifications. To further refine the accuracy with which MCNPX simulates elastic scattering of photons, photonuclear elastic scattering must also be added to the photonuclear database. These processes have been systematically studied by several groups and theoretical calculations are now in reasonable agreement with measured data [12, 13]. These physical processes can be added to ENDF via the same steps as have been used to add the NRF data. Upon adding these data to the photonuclear datafiles, we anticipate that MCNPX will be able to accurately simulate all physics processes relevant to modeling NRF for materials assay.

#### **4. Approach to Assay of Spent Fuel Assembly**

As with the single fuel pin assay, the goal in assaying a fuel assembly is to measure NRF rates within the assay volume, thereby determining the concentration of specific isotopes. However, NRF assay of an assembly introduces additional physical challenges; larger physical dimensions of the assembly cause more photon attenuation and assay of an entire spent fuel assembly induces proportionally higher radioactive intensities due to fission product decay.

To overcome these additional challenges, and to improve the NRF signal intensity relative to the background, the method considered here for assay of a fuel assembly uses an isotopically pure foil, referred to herein as a witness foil. A schematic describing the method is shown as figure 4. The witness foil is placed downstream to scatter photons that penetrate the assembly. Resonant energy photons that impinge upon the witness foil induce NRF and are subsequently re-emitted. Detectors located at backwards angles relative to the interrogating beam direction are significantly more likely to measure NRF  $\gamma$ -rays compared to other scattered photons. NRF that occurs within the assembly reduces additionally attenuates resonant energy photons as they are transmitted through the assembly subsequently reducing the rate at which resonant energy photons are measured by the detector array. The amount of the witness foil isotope contained within the assembly is correlated to the count rate reduction.

The witness foil method can dramatically reduce the fluence due to fission product activity at the detector location because detectors are positioned to view the witness foil rather than the spent fuel assembly. While assemblies attenuate more of the interrogating radiation, their larger dimensions also allow a larger fraction of the bremsstrahlung beam to be used for interrogation. By measuring transmitted photons this method also is uniformly sensitive over the entire sample volume irradiated by the interrogating photon beam.

<sup>235</sup> U Enrichment	$I_{\text{res}}/I_{\text{non-res}}$ Leaving Assembly	Relative Detector Count Rate
0.00%	1	1
0.50%	0.979	0.982
1.00%	0.959	0.963
5.00%	0.812	0.832

Table 2. Calculated relative intensities for resonant and non-resonant photons leaving the assembly (column 2) and impinging upon the photon detector (column 3). Values are for the homogenized assembly described in the text.

#### 4.1 Witness Foil Method Applied to Homogenized Assembly

To illustrate the witness foil method, a simplified problem is presented wherein the 1.733 MeV <sup>235</sup>U NRF signature is used to assay homogenized fuel assemblies with various enrichments. Photons are described as resonant or non-resonant. All photons are assumed to have identical photo-atomic interaction properties, but only resonant photons are assumed to undergo NRF.

Equal intensities (normalized per unit of energy) of resonant and non-resonant photons are impinged upon a homogenized assembly and attenuated by simple exponential attenuation over the 22 cm thickness of the assembly. The value of the attenuation coefficient was taken from the XCOM database [14] for a material mixture that represents a homogenized assembly of density (4 g/cm<sup>3</sup>). The attenuation coefficient for resonant photons is increased due to the addition of the NRF cross section (which is assumed to be constant for all resonant energy photons). The relative intensities of resonant photons are compared to the intensity of non-resonant photons in column 2 of table 2.

The exponentially attenuated photons then impinge upon the witness foil, a 1 mm thick slab of isotopically pure <sup>235</sup>U. The relative photon fluences due to resonant and non-resonant photons are calculated for an arbitrary detector position. For non-resonant photons, this fluence was only due to elastic scattering of photons and his cross section was assumed to be 100  $\mu\text{b/str}$ .

The witness foil is about  $2 \times 10^4$  times as likely to backscatter resonant photons as non-resonant photons. However, the ratio of detected resonant to non-resonant photons must be corrected for the energy resolution of an HPGe detector. Assuming a 3 keV resolution, the expected fluence of resonant photons is calculated to be 8.5 times that of non-resonant photons with no <sup>235</sup>U within the assembly. This ratio decreases to 6.8 for 5% <sup>235</sup>U enrichment.

The concentration of <sup>235</sup>U present within the fuel assembly is measured by observing the decrease count rate in a detector at the energy of the NRF resonance. Neglecting down-scattering from higher-energy photons, the relative decrease in detector count rate is shown in the third column of table 2. This indicates that for 0.5% and 5% <sup>235</sup>U enrichments, the NRF peak in the backscattered spectrum would decrease by 1.8% and 17%, respectively. The challenge for this method is accruing sufficient counting statistics such that these differences can reliably be observed.

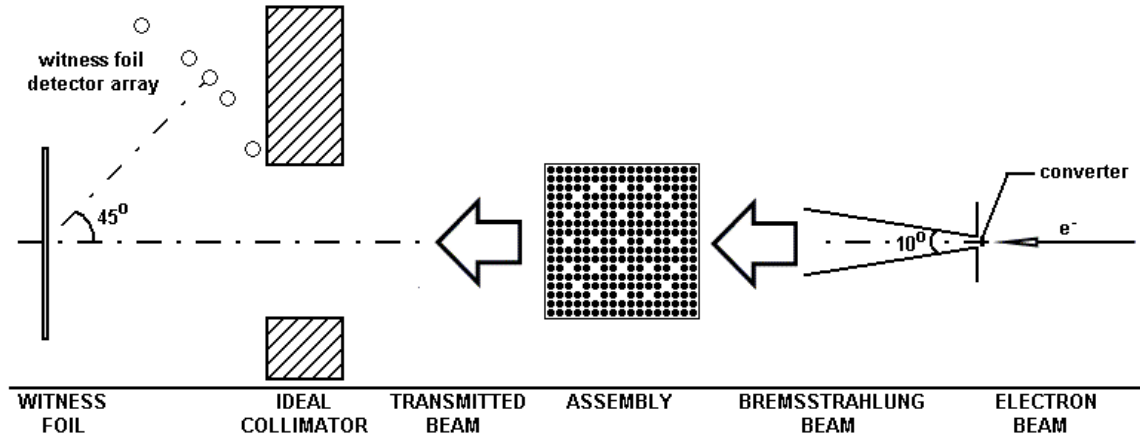


Figure 4. Schematic setup for MCNPX modeling of an assembly using the witness foil.

#### 4.2 Initial MCNPX Modeling of Assaying Assembly Using Witness Foil

Unlike the back-scattered photon spectrum, the transmission of photons through material *is* modeled accurately in MCNPX. Simulation of NRF assay setup was performed for a 17x17 pin PWR fuel assembly (figure 4). This assembly serves as a baseline case for the variety of NDA concepts currently in consideration as part of the spent fuel assay project [1,15]. The interrogation source is a bremsstrahlung beam obtained by impinging 2 MeV electrons upon a 4.5 mm thick tungsten converter. Photons emitted from the converter within 10° of the initial electron trajectory are transported through the fuel assembly. The solid angle of this collimated bremsstrahlung beam subtends the entire back plane of the assembly. Photons leaving the back plane of the assembly are collimated so that only photons within 4.3° of the initial electron beam can directly reach the witness foil, which has been modeled as a 5 mm thick cylindrical slab of isotopically pure  $^{235}\text{U}$ . A series of next event estimator tallies are placed between 120° and 170° relative to the initial beam direction. The assembly cross section is a square with 21.42 cm sides. The source is located 40 cm away from the assembly front side. The witness foil is located 80 cm from the back plane of the assembly and the detector array is 40 cm from the witness foil.

An example assay spectrum obtained from the simulation of the witness foil technique is shown in figure 5 for an assembly with 5%  $^{235}\text{U}$  enrichment. Although NRF physics is implemented in this MCNPX simulation, the elastic scattering processes, as described in section 3, were still missing. While the NRF peaks are clearly visible in the spectrum, it is anticipated that the photon continuum will increase by a large factor for the correct simulation of the background. Furthermore, the statistical uncertainty of NRF peaks within the spectrum remains large. This spectrum was generated by simulating  $1.5 \times 10^{10}$  bremsstrahlung photon histories. The run was conducted on 80 processors and lasted 24 hours. The number of simulated photons corresponds to less than 15 seconds of an actual interrogation with a bremsstrahlung beam produced by 100 $\mu\text{A}$  electron accelerator. Despite this lengthy run time, only 866 photons have contributed to the NRF peaks shown in figure 5. More elaborate variance reduction techniques are being considered to improve the efficiency for this type of MCNPX simulation.



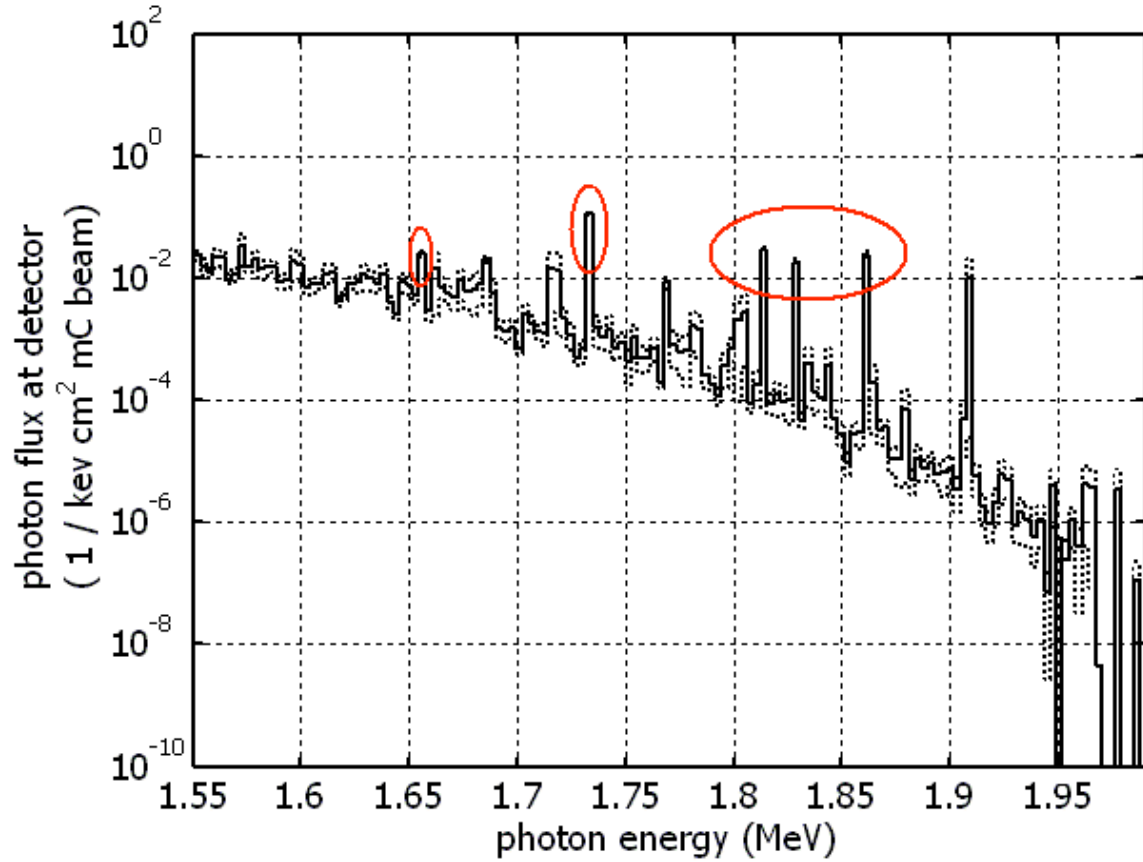


Figure 5. Spectrum calculated for 45° detector location indicated in figure 4. One standard deviation errors estimated by MCNPX are shown as dotted lines. Peaks due to NRF in  $^{235}\text{U}$  are circled.

## 5. Conclusions

NRF can, in principal, be used to quantify isotopic compositions of materials. The initial research approach investigated the method of measuring the NRF lines in  $\gamma$ -ray spectra emitted at backwards angles from spent fuel irradiated by a bremsstrahlung beam. The initial MCNPX simulations indicated high NRF signal to background ratios even for  $^{235}\text{U}$  and  $^{239}\text{Pu}$  concentrations well below 1% of the actinide mass in spent fuel. However, it was determined that MCNPX does not accurately calculate the dominant processes contributing to the background. Estimates based on published data indicate that the background is several times higher than the MCNPX results, thus limiting the sensitivity of NRF measurements at backward angles accordingly.

The signal-to-background ratio in this method is constrained by the energy resolution of the  $\gamma$ -ray detector (HPGe) which is roughly a thousand times lower than the Doppler-broadened width of the NRF lines. The method of using a witness foil to enhance the system response to resonant energy photons has been considered and simulation studies have been started. The complexity of measuring resonant energy photon penetration through a fuel assembly is the motivation for improving the photon scattering physics in MCNPX so that this assay method can be accurately modeled. NRF physics and a more complete treatment of Rayleigh scattering have been added to MCNPX and work is

continuing to implement photonuclear elastic scattering processes such as Delbruck and nuclear Thompson scattering as well.

## 6. Acknowledgements

This work is supported by an ARI grant from the National Science Foundation, the Department of Homeland Security BS123456, the Next Generation Safeguard Initiative of the Office of Nonproliferation and International Security (US DOE, NA-241), the Advanced Fuel Cycle Initiative of the Office of Nuclear Energy (US DOE) and by the Director, Office of Science of the US Department of Energy at the Lawrence Berkeley National Laboratory under contract number DE-AC02-05CH11231.

## 7. References

1. S. Tobin, "Determination of Plutonium Content in Spent Fuel with NDA – Why an Integrated Approach?," Annual Meeting of the Institute of Nuclear Material Management, Nashville, TN, 2008 (LA-UR-08-03763).
2. U. Kneissl et al. "Investigation of Nuclear Structure by Resonance Fluorescence Scattering," Prog. Part. Nucl. Phys. 37 1996, pp. 349.
3. G. Warren et al. "Nuclear Resonance Fluorescence of  $^{235}\text{U}$ ," IEEE Nuclear Science Symposium 2006, pp. 914.
4. W. Bertozzi et al. "Nuclear resonance fluorescence excitations near 2 MeV in  $^{235}\text{U}$  and  $^{239}\text{Pu}$ ," Phys. Rev. C. 78, 041601, 2008.
5. Pelowitz, J.F. (ed.), "MCNPX<sup>TM</sup> USER'S MANUAL Version 2.6.0," Los Alamos National Laboratory report LA-CP-07-1473 2008.
6. L. Kissel, Radiat. Phys. Chem. 59 2000, 185. Available: <http://adg.llnl.gov/Research/scattering/RTAB.html>
7. M.B. Chadwick, P. Oblozinsky, M. Herman et al., "ENDF/B-VII.0: Next Generation Evaluated Nuclear Data Library for Nuclear Science and Technology," Nuclear Data Sheets, vol. 107, pp. 2931-3060, 2006.
8. R. E. MacFarlane, NJOY 99 Nuclear Data Processing System, code available at <http://t2.lanl.gov/codes/njoy99/>
9. E.D. Cashwell et al. "Monte Carlo Photon Codes: MCG and MCP" LA-5157-MS, March, 1973.
10. D.E. Cullen, J.H. Hubbell and L. Kissel, "EPDL97: the Evaluated Photon Data Library, '97 Version", report UCRL-50400, Vol.6, Rev.5, 1997.
11. G. Hardie, W.J. Merrow, D.R. Schwandt, "Large-angle elastic scattering of 1.33-MeV photons from lead and uranium," Phys. Rev. C 1, 714–720, 1970.
12. G. Hardie, J.S. de Vries, C. Chiang, "Elastic scattering of 1.33-MeV photons from lead and uranium," Phys. Rev. C 3, 1287–1293, 1971.
13. P. Rullhusen, F. Smend and M. Schumacher, "Elastic Scattering of 2.754 MeV Photons by Ta and Interference between Rayleigh, Thomson and Delbrück Scattering," Z. Physik A 288, 119-123, 1978.
14. XCOM: Photon Cross Sections Database, NIST Standard Reference Database 8 (XGAM) <http://physics.nist.gov/PhysRefData/Xcom/Text/XCOM.html>
15. M. L. Fensin, S. J. Tobin, N. P. Sandoval, S. J. Thompson, M. T. Swinhoe, "A Monte Carlo Linked Depletion Spent Fuel Library for Assessing Varied Nondestructive Assay Techniques for Nuclear Safeguards," LA-UR 09-01188, ANS Advances in Nuclear Fuel Management IV, Hilton Head Island, SC (2009)